Journal of Power Sources 266 (2014) 374–383

Contents lists available at ScienceDirect

Journal of Power Sources

journal homepage: www.elsevier.com/locate/jpowsour

Polyvinylpyrrolidone as binder for castable supercapacitor electrodes with high electrochemical performance in organic electrolytes

M. Aslan [a], D. Weingarth [a], N. Jäckel [a], J.S. Atchison [a], I. Grobelsek [a], V. Presser [a, b, *]

[a] INM – Leibniz Institute for New Materials, Campus D2 2, 66123 Saarbrücken, Germany
[b] Saarland University, Campus D2 2, 66123 Saarbrücken, Germany

HIGHLIGHTS

- Polyvinylpyrrolidone (PVP) can be used as a binder in supercapacitors.
- PVP-electrodes can be casted or sprayed and used in organic electrolytes.
- PVP as a binder yields better performance as polyvinylidenedifluoride (PVDF).

ARTICLE INFO

Article history:
Received 19 February 2014
Received in revised form
11 April 2014
Accepted 10 May 2014
Available online 20 May 2014

Keywords:
Supercapacitor
Polymer binder
Casting
Electrode manufacturing

ABSTRACT

Polyvinylpyrrolidone (PVP) is presented as a "greener" alternative to commonly used supercapacitor binders, namely polyvinylidenedifluoride (PVDF) or polytetrafluoroethylene (PTFE). The key advantages of using PVP are that it is non-toxic and soluble in ethanol and it can be used to spray coat or drain cast activated carbon (AC) electrodes directly on a current collector such as aluminum foil – in contrast to PTFE that requires rolling or PVDF that requires toxic *N*-methylpyrrolidone (NMP). The electrodes with the best mechanical stability incorporated 3.5 mass% of 1.300.000 g mol^{-1} PVP. Compared to PTFE or PVDF, the resulting pore volume was significantly higher and the specific surface area significantly larger when using PVP (normalized to the amount of AC). A good electrochemical performance was observed in organic electrolytes for AC–PVP electrodes: 112 or 97 F g^{-1} at 0.1 A g^{-1} in 1 M TEA–BF_4 in propylene carbonate or acetonitrile, respectively. The performance stability was comparable to PTFE-bound electrodes when adjusting the maximum cell voltage to 2.5 V while preserving the manufacturing features of PVDF–AC films. (Electro)chemical stability is shown by electrochemical testing and infrared vibrational spectroscopy for propylene carbonate and acetonitrile.

1. Introduction

Limited availability of fossil fuels and the sustainable transition of our transportation fleet to electric cars have greatly expedited the research activities related to the large scale implementation and generation of energy from renewable resources. To achieve the ambitious goal of 15–20% of renewable energy for the total electricity supply in the coming years set by many countries worldwide, not only technologies for energy generation and transport are needed, but grid stability and efficiency greatly require advanced energy storage technologies [1,2]. Among energy storage solutions, electrical double layer capacitors (EDLCs), also called ultra- or supercapacitors, have emerged as a particularly promising technology that is already widely used in commercial consumer electronics, memory back-up systems, and industrial power and energy management systems [3–5]. Based on non-faradaic energy storage via reversible ion electroadsorption, EDLCs excel in long lifetime, fast charge/discharge rates, and high power density, while maintaining a moderate energy density compared to state-of-the-art lithium ion batteries [6–8].

A typical EDLC consists of two electrodes composed of porous carbon, which are spaced by an electrically isolating porous separator immersed in an electrolyte (aqueous/organic/ionic liquid based), all of which are contained in a metal housing. [9] One key component is the active electrode material, which is typically bound by a polymeric binder to form mechanically stable and coherent films. Activated carbons (AC) are the most commonly used active material due to their large surface area, sufficient electrical conductivity, natural abundance of precursors, and availability at moderate cost [1,10].

* Corresponding author. INM – Leibniz Institute for New Materials, Campus D2 2, 66123 Saarbrücken, Germany.
E-mail address: volker.presser@inm-gmbh.de (V. Presser).

http://dx.doi.org/10.1016/j.jpowsour.2014.05.031
0378-7753/

To be used in an EDLC device, self-standing electrode sheets or AC coatings have to be applied to metallic current collectors (typically carbon coated aluminum) [9]. For the preparation of such electrodes, AC powders are mixed with suitable polymer binders such as polytetrafluoroethylene (PTFE) or polyvinylidenedifluoride (PVDF) in an amount typically between 5 and 10 mass% [9,11,12]. While being highly suitable to craft free-standing carbon/polymer film electrodes, PTFE prohibits direct casting onto metal current collectors. However, improved material integrity at the active material/current collector interface may enhance the electrochemical performance for electrode systems directly attached to the current collector. PVDF is widely used for this purpose because of its chemical inertness and suitability of the rheological properties of the carbon slurry [13]. Yet, to obtain coatings of sufficient mechanical stability, high amounts of PVDF have to be added (around 10 mass%) which increases the dead mass and potentially reduces the overall capacitance of the device by blocking access to the pore network [14]. Moreover, there are growing concerns regarding the use of PVDF because of the necessary addition (and subsequent removal) of *N*-methyl-2-pyrrolidone (NMP) during electrode preparation which is a dipolar aprotic solvent classified as a reproductive toxicant [15]. In addition, the way of blending the electrode material with binder impacts the electrochemical performance as binder may obstruct the access of ions to a significant portion of the total surface area and the defragmentation of carbon particles may cause an increase in electrical resistance [16]. Indeed, based on data of free-standing binder-free electrodes, it would be preferential to avoid the use of any binder [17–19]. However, this is in most cases not possible as it would exclude the use of highly available and cost-attractive activated carbon powders.

The selection of binder material has to balance a couple of partially diametrical properties. It is especially important to lower the amount of added binder as they are commonly electrically insulating and do not contribute to the charge storage mechanism. In particular, the challenge is to combine chemical stability in the presence of the selected electrolyte, mechanical strength, and film integrity with little or no detrimental impact on either particle porosity or electrical film conductivity. Furthermore, with environmental awareness driving the selection of supercapacitor components, interest has also increased in investigating "green" or "greener" materials and especially fluorine free binders [13,14,20]. In particular, carboxymethylcellulose (CMC) has been introduced as a promising binder material [21,22]; yet, to enable a high capacitive performance, chemical modification of CMC or the addition of PTFE is required that renders this interesting material rather elaborate and expensive in its application to EDLC devices [23]. Natural cellulose has also been investigated as a "green" binder material; however, this material usually requires large amounts of added conductive additive to obtain an adequate rate handling [24]. Work on fuel cells and carbon nanotube surfactants indicates that polyvinylpyrrolidone (PVP) may also be a promising fluorine-free binder for non-aqueous electrolytes (PVP dissolves in water) [25,26]. Until now, there has been no systematic study using PVP as a binder for EDLC electrodes that includes its effect on mechanical strength, the electrical conductivity of the electrodes, and the resulting electrochemical performance.

In our study, a parametric and comprehensive evaluation of different types of PVP as a binder for EDLC electrodes for non-aqueous electrolytes will be presented. The striking advantage of PVP-based electrodes is that they can be coated directly onto metallic current collectors by casting or spray coating. This enables scalable application in a cost sensitive industrial production where currently PVDF is employed; yet, unlike PVDF, no toxic solvent is required for electrode fabrication. The obtained film electrodes were tested in a symmetric two electrode cell geometry using standard electrolytes, that is, 1 M tetraethylammonium tetrafluoraborate (TEA–BF_4) in either acetonitrile (ACN) or propylene carbonate (PC). The electrochemical performance is investigated using cyclic voltammetry and constant voltage floating, whereas the chemical stability is determined using infrared spectroscopy. The properties are compared to conventional binder materials, namely PTFE and PVDF.

2. Experimental description

2.1. Reagents

Activated carbon (AC) powder (YP50-F, Kuraray Chemical) was used as the active material for the preparation of EDLC electrodes. Polyvinylpyrrolidone (PVP, Sigma Aldrich) of different molecular masses was used as dispersant/binder. The molecular mass of PVP was 40.000, 360.000, and 1.300.000 g mol^{-1} as reported by the manufacturer. In addition to PVP, also PVDF and PTFE (as a 60 mass% aqueous solution, Sigma Aldrich) were used. Tetraethylammonium–tetrafluoroborate (TEA–BF_4) was used in 1 M solution in propylene carbonate (PC) or acetonitrile (ACN; all purchased from BASF Battery Materials). The water of both solvents was below 20 ppm as confirmed by Karl Fischer titration.

2.2. Electrode preparation

Slurries with PVDF binder were prepared by the following procedure: 0.2 g of PVDF powder was dissolved in 8 g of *N*-methyl-2-pyrrolidone, NMP, from Sigma–Aldrich in an oil bath at 100 °C under constant stirring. Afterward, 1.8 g of AC powder was added and the mixture, which was stirred for 10 min at room temperature and then for another 15 min in an ultrasound-assisted ice bath. The resulting slurry consisted of 10 mass% solid fraction with respect to the total mass (i.e., AC plus PVDF). For the ultrasound treatment, a Branson Sonifier 450 with a maximum power output of 400 W was used (duty cycle: 20%, output power: 30%).

For the electrodes with PVP binder ethanolic slurries containing AC powder and different amount of PVP with a solid content of 20 mass% with respect to total mass (i.e., AC plus PVP plus ethanol) were prepared by ultrasound-assisted stirring in an ice bath for 10 min with parameters as described above. The amount of PVP in the AC–PVP slurries was varied between 2.5 and 5 mass% with respect to the mass of PVP plus AC. The PVDF containing slurry was drain casted directly on the aluminum current collector (30 μm thickness, Carl Roth) and AC coatings of 50–70 μm thickness were obtained. Afterward the aluminum foils coated with AC–PVDF were dried at 80 °C in an air recirculating oven at ambient pressure for 10 h followed by a drying step at 120 °C under 20 mbar vacuum for 24 h. After mixing, the PVP containing slurry was transferred in a nitrogen filled glove box (O_2, H_2O < 0.1 ppm, MBraun, Germany), where it was drain casted on carbon coated aluminum current collector foils (type Zflo 2653, Exopack technologies). A coating thickness of 50–70 μm was achieved. The AC–PVP foils were dried in one step at 90 °C for 2 h on a heating plate inside the glove box.

The AC–PTFE electrodes were prepared by the following procedure: A mixture of 2.375 g AC powder and 0.208 g of aqueous PTFE solution were homogenized in a mortar and pestle by adding drops of ethanol to a dough-like mass resulting in AC–PTFE mixtures with 5 mass% PTFE with respect to AC plus PTFE. These prepared AC–PTFE mixtures were rolled into free standing 100 μm thick foils by a twin roller (MTI HR01, MTI Corporation) and were dried at 120 °C in vacuum at 20 mbar for 24 h.

2.3. Mechanical and structural characterization

Mechanical testing of the coatings was done with a micro scratch tester (MST) within 30–1000 mN at a loading rate of 970 mN min^{-1} and a speed of 10 mm min^{-1} (CSEM Centre Suisse d'Electronique et de Microtechnique SA). In this method, a 400 μm diameter diamond ball is sliding on the coating at a given speed (10 mm min^{-1}) with a load rate of 970 mN min^{-1} (test length: 10 mm, start load: 30 mN). The position of the ball, penetration depth, and the load were recorded.

Scanning electron microscopy (SEM) was used to investigate the particle morphology and film consistency. A JSM-7500F (JEOL) field-emission system operating at 2 or 5 kV was used and the films were studied without the application of a conductive sputter coating.

Specific surface area (SSA) and pore size distribution of the carbon powder and binder-containing films were determined by N_2 sorption measurements at 77 K (Autosorb 6B, Quantachrome Instruments) using the quenched solid density functional theory (QSDFT) kernel implemented in the AS1WIN software package from Quantachrome Instruments. [27] The isotherms were fitted assuming a slit pore shape. BET SSA (Ref. [28]) was determined within the partial pressure range between 0.0016 and 0.05 P P_0^{-1} that yielded the best linear correlation for the BET equation [29,30].

Raman spectra were measured with a Renishaw inVia system employing a laser operating at 532 nm (<2 mW) focused with a 50× objective lens with a numeric aperture of 0.9. Raman spectra were recorded with a lateral resolution (in the focal plane) of circa 2 μm and a spectral resolution of ~1.2 cm^{-1}.

The attenuated total reflection Fourier transform infrared (ATR FTIR) spectroscopy was performed with a Bruker Tensor 27 single bounce diamond ATR system. The spectral resolution was set to 16 cm^{-1} and spectra were averaged over 64 scans. Scans of the individual chemicals were background subtracted using the recorded IR spectrum of air and the spectra taken with the electrodes were corrected using a measurement of pure AC as the background. All background spectra were taken at the same resolution (16 cm^{-1}) averaged over 32 scans. Care was taken to expose the samples to ambient conditions for less than 10 s before (23 °C, 31% relative humidity) taking the spectra. The time series studies were accomplished by placing a drop of electrolyte on the electrode and inverting the electrolyte-carbon-polymer system and sealing the sample under an aluminum foil with the ATR anvil. In this configuration, water absorption by the sample is inhibited and trace amounts of water in the sample came only from the brief exposure to ambient conditions during the insertion of the sample on the ATR crystal.

2.4. Electrochemical characterization

The electrical conductivity of the samples was determined by four point probe measurements using a custom-built system. Four spring loaded gold pins are in contact with the electrode material and a highly sensitive Ampère-meter (Prema 4001 Digital-multimeter) was used to determine the film resistance. The 1.5 mm diameter tips were flat and had a tip-to-tip spacing of 3.0 mm.

The electrochemical characterization was carried out in a custom-built spring-loaded test cell corresponding with the setup reported in Ref. [31]. Electrodes of 12 mm diameter were punched out of the prepared electrode sheets and used in symmetric two-electrode cells using a glass fiber separator of 13 mm diameter and 260 μm thickness (GF/A, Whatman). The cell assembly was done in an argon filled glove box (O_2, H_2O < 0.1 ppm, MBraun). Electrochemical characterization in symmetric cells consisted of cyclic voltammetry (CV) measurements at different scan rates (1, 10, 50, and 100 mV s^{-1}) up to 2.7 V cell voltage with 10 s resting (at 0 and 2.7 V, respectively) for performance testing and galvanostatic charge and discharge with potential limitation (GCPL)

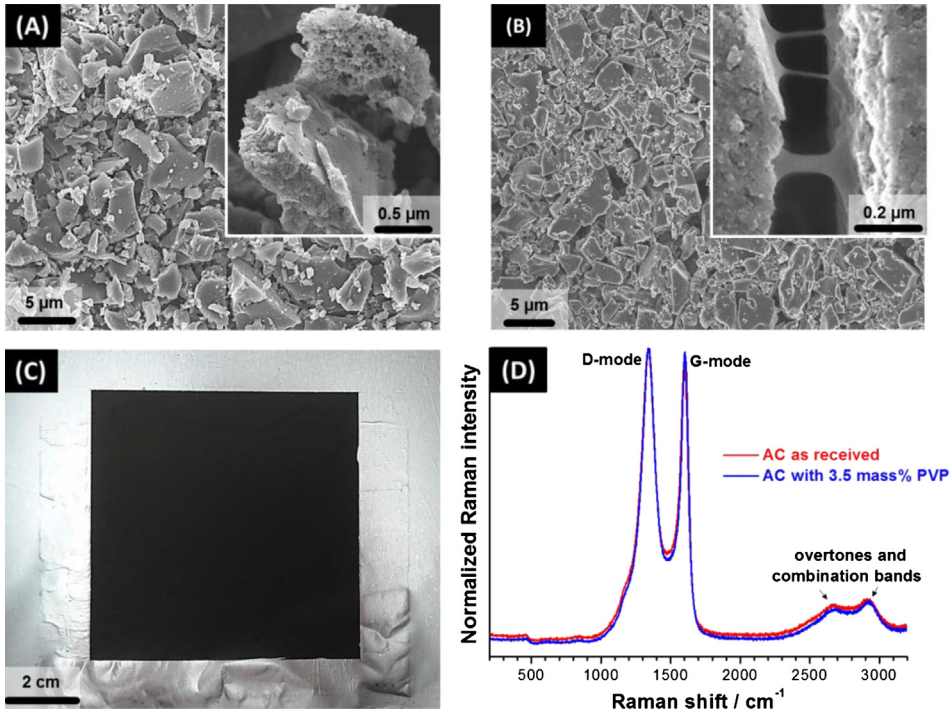

Fig. 1. (A–B) Scanning electron microscope images (SEM; acceleration voltage: 5 kV except 2 kV for the inset in B) of activated carbon (AC) powder particles. (A) Dry powder. (B) Casted AC electrode on aluminum using 3.5 mass% of polyvinylpyrrolidone (PVP). (C) Photograph of the casted electrode on aluminum (10 × 10 cm^2). (D) Raman of the as received AC powder and the PVP-bound electrode.

measurements for constant voltage aging experiments as described in more detail in Ref. [32]. The long term stability of the electrode materials was tested at a constant voltage of 2.5 V or 2.7 V (floating) and in 10 h intervals, the electrodes were discharged and three cycles to 2.5 V are performed to determine the capacitance; this procedure was repeated for ten times. In all experiments, only the discharge current was used for the calculation of the specific capacitance [33]. A detailed investigation of the electrochemical stability window of AC–PVP electrodes was done according to Ref. [34]. For that the counter electrode (PTFE bound YP50) was largely oversized in charge capacity and a reference electrode prepared from YP50 was attached to the system from the side [31,35]. The potential window opening was conducted from 0.3 V vs. carbon to 2.5 V vs. carbon in 100 mV steps. The negative potential window was investigated in a separate cell with the same potential step size, respectively. All electrochemical experiments were carried out using a VSP-300 potentiostat/galvanostat (Bio-Logic Science Instruments).

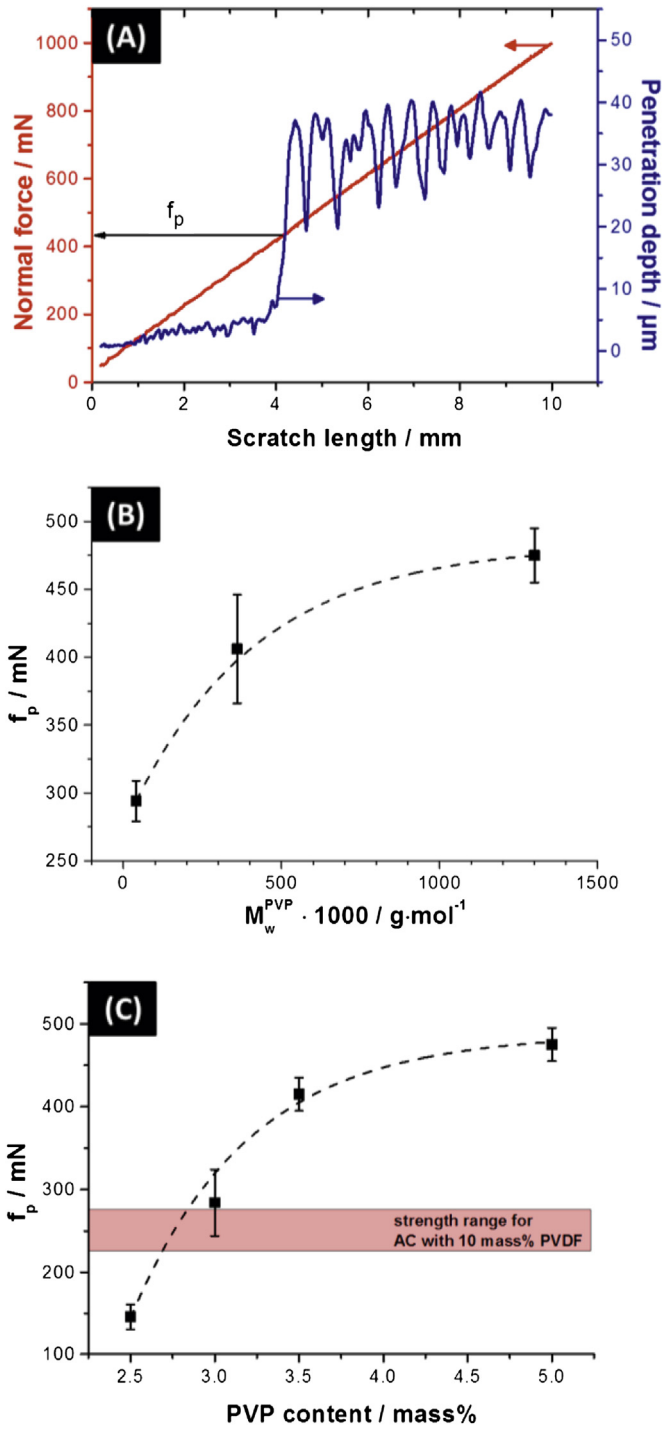

Fig. 2. (A) Typical micro scratch measurement on activated carbon (AC) electrodes. (B) Influence molecular mass (M_w) of polyvinylpyrrolidone (PVP). (C) Influence of PVP content.

3. Results and discussion

3.1. Structural characterization of AC

The used AC powder consisted of agglomerates of porous particles with a size ranging from below 1 to circa 10 µm (Fig. 1A). After casting on aluminum current collector, the AC–PVP film showed optical and morphological film integrity and high resolution imaging shows evidence for particle–particle gluing (Fig. 1B). Electrodes with an area of >100 cm^2 were coated, as outlined in the experimental section, directly on the current collector (Fig. 1C; example shown: 100 cm^2).

Raman spectra indicate that the carbon powder is composed of incompletely graphitized carbon, as seen from the emergence of both, a disorder related D-mode (1343 cm^{-1}) besides the G-mode (1605 cm^{-1}) which is related to a sp^2-hybridized carbon network (Fig. 1D) [36,37]. The addition of 3.5 mass% PVP (molecular mass: M_w = 1.300.000 g mol^{-1}) to the carbon material does not induce any change to the Raman spectrum and, as expected from the ambient-temperature treatment process, no change to the carbon structure (i.e., the I_D–I_G ratio remains at a value of 1.54 ± 0.02 using Lorentzian peak fitting).

3.2. Influence of the binder on mechanical and electrical properties and porosity

PVP is available in different molecular masses and it is important to study the possible impact of M_w on the resulting film properties (especially considering film integrity and strength). For that, coatings were derived from carbon slurries by drain casting with 5 mass % of PVP with varying M_w-values and tested using a micro scratch tester. In such experiments, the load corresponding to the sudden increase of the measured penetration depth is defined as penetration force, f_p, which describes the mechanical performance of the coatings as illustrated for a typical measurement in Fig. 2A.

Table 1
Pore characteristics (specific surface area, SSA; volume-weighted average pore size, d_{50}; total pore volume) obtained from nitrogen gas sorption analysis at 77 K using the BET equation and quenched solid density functional theory (QSDFT) assuming a slit pore shape for activated carbon (AC) with or without the addition of polymer binder (polyvinylpyrrolidone, PVP; polytetrafluorethylene, PTFE; polyvinylidenedifluoride, PVDF).

	SSA (m^2 g^{-1})		Average pore size[b] (nm)	Pore volume (cm^3 g^{-1})
	BET[a]	QSDFT	QSDFT	QSDFT
AC as received	1720	1521	0.94	0.73
AC with 3.5 mass% PVP	1675	1485	0.93	0.71
AC with 5 mass% PVP	1574	1392	0.94	0.66
AC with 5 mass% PTFE	1523	1330	0.96	0.65
AC with 10 mass% PVDF	1213	1031	0.99	0.52

[a] BET SSA derived from the linear region between 0.0016 and 0.05 P P$_0^{-1}$.
[b] Average pore size refers to the volume-weighted average pore size, d_{50}, derived via $d_{50} = \sum_{i=1}^{n} d_i \cdot V_i / \sum_{i=1}^{n} V_i$ with d as the pore size and V as the pore volume.

Using a fixed amount of PVP binder (i.e., 5 mass%) with different molecular mass significantly affects the penetration force (Fig. 2B). Increasing M_w from 40.000 to 360.000 to 1.300.000 g mol^{-1}, the penetration force increases from 294 to 406 and 475 mN (corresponding to an improvement of 161%). This is in agreement with the observation of other PVP composites that showed improved mechanical properties for increased molecular mass [38]. From these results we concluded to use PVP with a molecular mass of 1.300.000 g mol^{-1} for the remainder of the study.

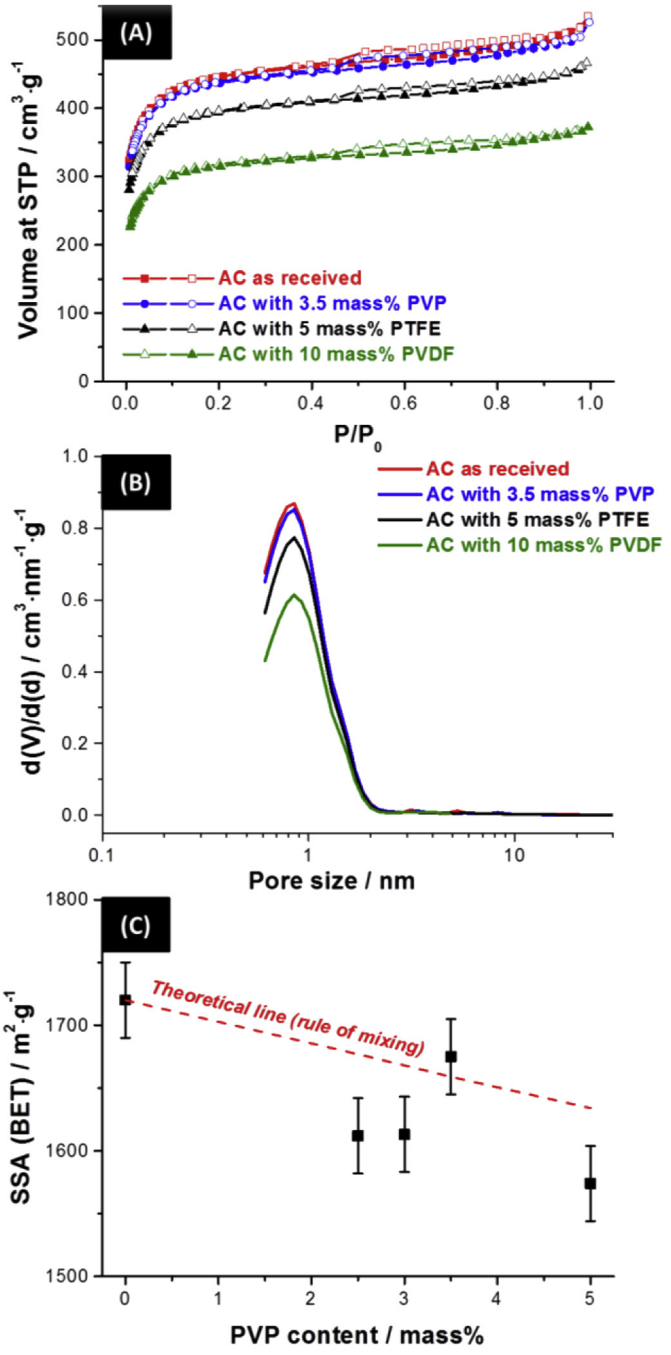

Fig. 3. (A) Nitrogen sorption isotherms at 77 K of as received activated carbon (AC) with or without the addition of polymer binder (3.5 mass% of polyvinylpyrrolidone, PVP; 5 mass% of polytetrafluorethylene, PTFE; 10 mass% of polyvinylidenedifluoride, PVDF). (B) Quenched solid density functional theory (QSDFT) isotherm deconvolution of AC (pore size distribution). (C) Dependency of the specific surface area (SSA; derived from the BET equation) on the PVP content.

One key aspect of binder optimization strategies for EDLC electrodes is the minimization of binder content to balance optimized mechanical integrity (at higher amounts of binder) and electrical conductivity/reduced dead mass (at lower binder additions). Here, we varied the PVP content between 2.5 and 5.0 mass% and observed a constant increase in the penetration force at larger amounts of added binder (Fig. 2C). The best improvement in mechanical properties can be seen when increasing the PVP addition from 2.5 to 3.5 mass% (f_p: +184%) with only slight increase in f_p when even higher amounts of PVP were used (from 3.5 to 5 mass%; f_p: +14%). Compared to the commonly used PVDF (f_p: 253 ± 32 mN using 10 mass% of binder), PVP films with a content of only 3.5 mass % of binder show significantly better mechanical performance (f_p: 415 ± 20 mN). Thus, at lower binder concentration, higher film strength can be obtained; therefore, 3.5 mass% of PVP was used for the remainder of the study (unless otherwise stated). A comparison with only 5 mass% PVDF was not possible because of very low film integrity when using less than 10 mass%, and a comparison with PTFE-bound electrodes was not meaningful since PTFE-bound cannot be casted directly onto the current collector.

Another important aspect is the impact of binder to the film electrode porosity. It is a common misperception to use the porosity of dry powders of porous carbons to correlate with the electrochemical properties and not the porosity of the carbon film electrode which is actually measured. Usually, the difference between the porosity of dry powder with and without binder are not drastic, but noteworthy, because some of the total pore volume is blocked by the binder [14]. Table 1 provides an overview of the porosity (SSA, average pore size, and pore volume) of as received AC and compares the resulting pore characteristics for 3.5 and 5 mass% PVP, 5 mass% PTFE, and 10 mass% PVDF. The lowest PTFE binder content that still yielded mechanically coherent film electrodes in our experiments was 5 mass%.

Dry AC powder showed a BET SSA of 1720 m^2 g^{-1} (QSDFT SSA: 1521 m^2 g^{-1}), a total pore volume of 0.73 cm^3 g^{-1} dominated by micropores, and a volume-weighted average pore size (d_{50}) if 0.94 nm. When adding 5 mass% of PTFE or 10 mass% of PVDF, the total pore volume is decreased by 11 or 29%, respectively, due to a smaller amount of accessible micropores. These amounts greatly exceed the actual contribution of the PTFE or PVDF binder content

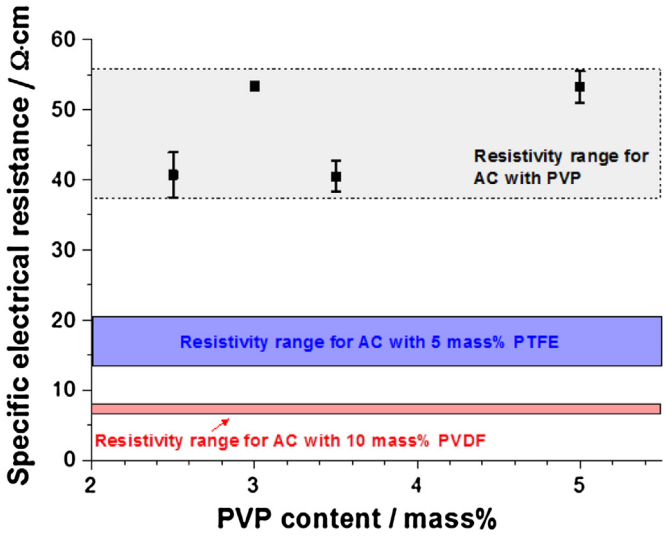

Fig. 4. Specific sheet electrical resistance, Ω cm, of various additions of polyvinylpyrrolidone (PVP) to activated carbon (AC). For comparison data is added for film electrodes with 10 mass% polyvinylidenedifluoride (PVDF), and 5 mass% of polytetrafluorethylene (PTFE).

(i.e., 5 or 10 mass%, respectively, of a material with essentially no specific surface area) and must be related to pore blocking. In contrast, only ≈3% of the pore volume is blocked by the binder when employing 3.5 mass% of PVP and this value is almost identical to the added mass of non-porous binder. Thus, PVP glues the AC particles together without actually blocking access to the high surface area and pore volume of the porous carbon. Consequently, the other pore characteristics remain almost unchanged when using 3.5 mass% of PVP compared to the dry powder (QSDFT SSA: −2%; average pore size: −0.1 Å) as can be expected from the minute differences to the nitrogen sorption isotherm at 77 K of the as received AC powder (Fig. 3A). Also in case of pore blocking for PVDF and PTFE with significantly decreased pore volume and surface area, the shape and type of the isotherm curve (type IV with a H4 hysteresis loop) [39,40] remain similar to the original AC powder, which results in almost no change of the pore size distribution (PSD, Fig. 3B) of the film electrodes. It is important to note that the adherence to a simple rule of mixing (i.e., negligible pore blocking and pronounced particle–particle-cohesion) is also observed to a large degree when increasing the PVP content up to 5 mass% (Fig. 3C). The ideal line of mixing was determined by using the mass fraction of AC and PVP and multiplying these amounts with the measured SSA values (i.e., AC: 1720 $m^2\ g^{-1}$; PVP: 4 $m^2\ g^{-1}$).

Besides the coherent mechanical stability and beneficial porosity, the electric conductivity is a key property of the composite electrode material. Within the studied range of 2.5–5.0 mass % of PVP added to AC, the resistance varies in the range from 38 to 55 Ω cm without any indication of a trend within the range of statistical scatter (Fig. 4). This value is appreciably higher than for the 10 mass% PVDF casted electrodes (ca. 8 Ω cm; i.e., lower by a factor of 5–7) possibly due to the improved particle–particle contact (that, however, did not translate to a better mechanical film integrity as seen previously).

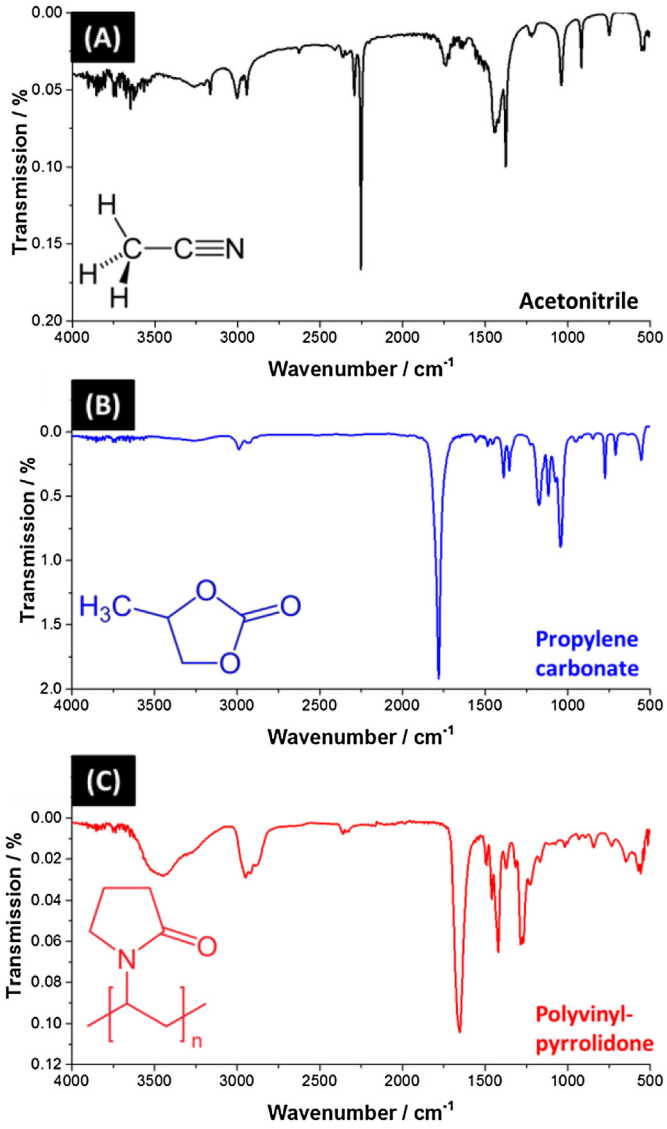

Fig. 5. Fourier transform infrared spectra (FTIR) using attenuated total reflectance (ATR) of (A) acetonitrile (ACN), (B) propylene carbonate (PC), and (C) polyvinylpyrrolidone (PVP) including their chemical structures.

3.3. Chemical compatibility of AC–PVP electrodes with organic electrolytes

While PTFE and PVDF are commonly used binder materials for EDLC electrodes using organic electrolytes, we have yet to establish chemical stability of PVP with ACN and PC to provide a basis for subsequent electrochemical testing. We also note that the use of aqueous electrolytes is excluded for PVP because of its high solubility in water. First, FTIR spectra were collected of the electrode films immersed in either ACN or PC (Fig. 5A–B) along with a casted AC electrode with 3.5 mass% PVP (Fig. 5C). A detailed list of assigned peaks can be found in Table 2. Note that the characteristic carbonyl

Table 2
FTIR peak assignment (polyvinylpyrrolidone, PVP; [41] propylene carbonate, PC [46]); acetonitrile, ACN [47]).

Chemical compound	Peak (cm^{-1})	Assignment	Notes
PVP	3500–3200	N–H stretch	Shifted broad peak due to hydrogen bonding
	3000–2800	CH_3–CH_2 stretch	
	1651	C=O	Typically seen at 1680 cm^{-1} down shifted due to hydrogen bonding
	1492	(Ring) CH_2 scissor	
	1456	(Ring) CH_2 scissor	
	1423	(Ring) CH_2 scissor	
	1374	C–H deformation	
	1016	C–C backbone	
	930	C–C ring breathing mode	
PC	2987	CH stretch	
	2928	CH stretch	
	1779	C=O	
	1559	Ring C–C	
	1484	Ring C–C	
	1453	Ring C–C	
	1227	C–O	Ester (attached to carbonyl)
	1387	CH_3 bending	
	1349	CH_3 bending	
	1075	C–O	Backbone
ACN	3170	CN	
	3004	C–H asymmetric stretch	
	2970	C–H stretch	
	2940	C–H stretch	
	2624	C–H stretch	
	2291	C–H bend	
	2250	CN stretch	
	1436	Asymmetric C–H bend	
	1412	C–H rock and C–N bend	
	1378	C–H bend	
	1035	CH_3 rock	
	917	Triple bond bending	
	752	Triple bond bending	
	545	Triple bond bending	

peak for PVP is typically found at 1680 cm^{-1} while it is located at 1651 cm^{-1} in our samples. The carbonyl peak in the PVP molecule is very sensitive to hydrogen bonding and when even minute amounts of water are present, the carbonyl peak can down shift [41].

The pristine AC–PVP electrode casted on aluminum did not show strong PVP peaks itself due to non-ideal contact with the ATR crystal and the opaque carbon matrix (Fig. 6A). Exposing the AC–PVP film electrodes on aluminum to PC did not result in significant changes in the vibrational spectra suggesting the AC–PVP–PC system is chemically very stable at room temperature (time series over 25 × 60 s is provided in Fig. 6B). A different situation can be observed when exposing AC–PVP electrodes casted on aluminum to ACN (Fig. 6C). Initially the spectra have the characteristic peaks associated with ACN; yet, as time progresses, the ACN peaks in the low wavenumber range disappear and peaks grow in the high wavenumber section. Additionally there is a growing C–O peak centered at (2380 cm^{-1}) not seen in any of the other spectra. This peak is a reaction by-product and not an artifact of the experimental conditions. Additionally, the growing peaks at 3350 and 3200 cm^{-1} are assigned to stretch vibrations of N–H, intermediate amines from the hydrolysis of acetonitrile, indicating the presence of minute amounts of water in the system (most probably ad- or absorbed by PVP). In the presence of water, ACN reacts to form acetamide releasing H_2 and CO_2 as reaction by-products [42]. The time series taken of the ACN on the PVP–AC electrodes reveals the loss of the ACN peaks (3000, 2293/2245, 1440/1375, 1040, 920, 748 cm^{-1}) and the growth of peaks between 3550 and 3200 cm^{-1} coupled with the peak at 1640 cm^{-1} indicating that hydrolysis has occurred. Yet, no degradation of the PVP itself is observed. However, it is important to note that the exact same mechanism of ACN hydrolysis is observed when ACN is studied directly on the FT-IR ATR crystal (Fig. 6D). Thus, it can be concluded that besides the well-known reaction of ACN with trace amounts of water which are adsorbed on the electrode, no further degradation mechanism would in principle contradict the suitability of PVP–AC for either ACN or PC electrolytes. To exclude the detrimental effect of water to the electrolyte stability, the PVP electrodes used in the next section were completely prepared inside the glove box with moisture and oxygen levels below 1 ppm.

3.4. Electrochemical measurements

Based on the results for mechanical stability and electrical conductivity/porosity measurements, we chose to carry out the electrochemical characterization of AC–PVP electrodes containing a binder content of 3.5 mass%. The coating thickness was in the range of 50–70 μm. Cyclic voltammetry (CV) was performed at scan rates 1, 10, 50, and 100 mV s^{-1} up to a cell voltage of 2.7 V for AC–PVP in 1 M TEA–BF_4 in either ACN or PC (Fig. 7A and B, respectively). Operating in PC, rectangular shaped CVs were obtained that showed a decrease in specific capacitance with increasing scan rate as a result of the more resistive behavior at higher power conditions. In contrast, pronounced faradaic reactions resulting in a distorted CV shape are encountered at a scan rate of 1 mV s^{-1} when the cell voltage approaches circa 2.5 V in ACN. These features vanish as soon as the scan rate is increased as the time during which the system remains at critical voltages is too short considering the apparently slow electrochemical reactions. Yet, it is clear from these results that 2.7 V in a symmetrical cell with two identical electrodes may be to too large for ACN (see also Fig. 8).

To evaluate the power handling, we performed galvanostatic charge and discharge sweeping from 0.1 to 10 A g^{-1} current density (Table 3, Fig. 7C). Using PC, the highest capacitance at 0.1 A g^{-1} was

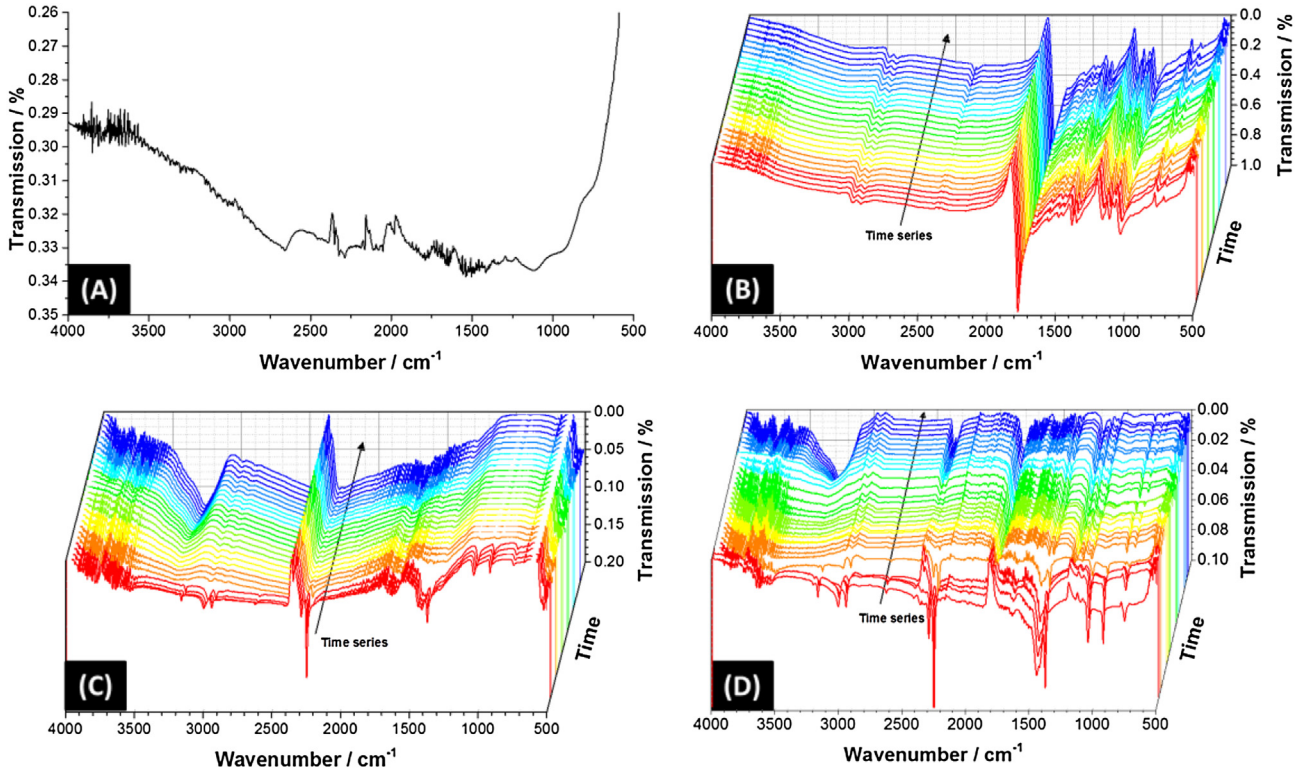

Fig. 6. (A) Fourier transform infrared spectroscopy (FTIR) spectrum of activated carbon (AC) film electrode containing 3.5 mass% polyvinylpyrrolidone (PVP). The background was corrected for the signal of pure carbon (dry AC). (B) Time series (25 × 60 s) for AC–PVP in propylene carbonate (PC). (C) Time series (25 × 60 s) for AC–PVP in acetonitrile (ACN). (D) Time series (25 × 60 s) for only the aluminum foil in ACN measured under ambient conditions (i.e., access of moisture).

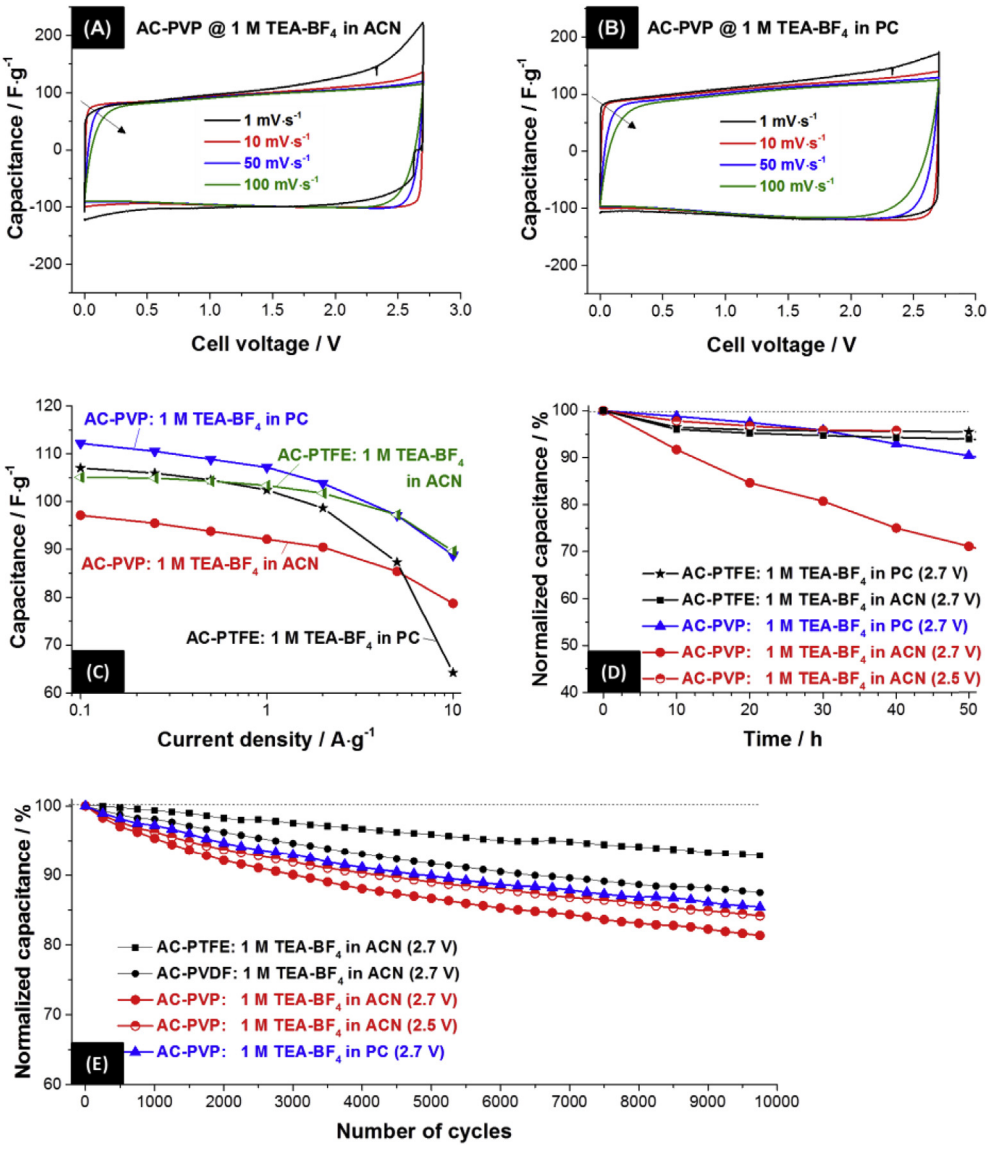

Fig. 7. Cyclic voltammograms (CVs) of an activated carbon (AC) film electrode with using 3.5 mass% polyvinylpyrrolidone (PVP) employing (A) acetonitrile, ACN, or (B) propylene carbonate, PC, with 1 M TEA–BF_4 as the salt in both cases. The arrows indicate the order in which the scan rate was increased from 1 to 100 mV s^{-1}. (C) Galvanostatic charge and discharge plots for AC–PVP and electrodes with 5 mass% of polytetrafluorethylene (PTFE). (D) Voltage holding at 2.5 or 2.7 V for 60 h. (E) Galvanostatic charge and discharge cycling at 1 A g^{-1} up to 2.5 or 2.7 V.

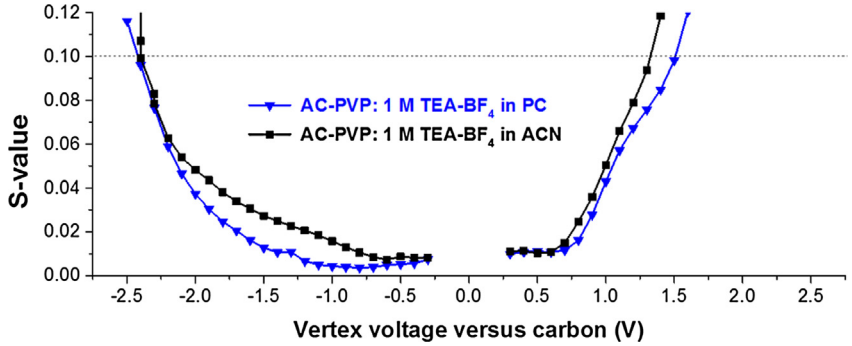

Fig. 8. Calculated S-values of an activated carbon (AC) film electrode using 3.5 mass% polyvinylpyrrolidone (PVP) casted on aluminum in a three electrode cell employing acetonitrile, ACN, or propylene carbonate, PC, with 1 M TEA–BF_4. Only a zoom in onto the range up to $S \leq 0.12$ is shown.

Table 3
Electrochemical performance of activated carbon (AC) electrodes with different binders in 1 M TEA–BF_4 (tetraethylammonium tetrafluoroborate) in propylene carbonate (PC) or acetonitrile (ACN) derived at 0.1 A g^{-1} using galvanostatic charge and discharge.

	Solvent	Specific capacitance (F g^{-1})
AC with 3.5 mass% PVP	PC	112
AC with 3.5 mass% PVP	ACN	97
AC with 5 mass% PTFE	PC	107
AC with 10 mass% PVDF	PC	70

measured for AC–PVP (112 F g^{-1}) followed by AC–PTFE (107 F g^{-1}) and AC–PVDF (70 F g^{-1}), while for ACN, we measured a value of 97 F g^{-1}. This slightly lower value (−15% compared to AC–PVP in PC) may be associated with the onset of electrochemical degradation when charging up to 2.7 V cell voltage but is much more significant than the difference to using 10 mass% PVDF (−38%). The decreased capacitance when using PVDF is a result of the reduced amount of available surface area. Staying within the range of values for PVP electrodes, it is important to note that there is a minimal variation and a very high reproducibility from batch to batch and when comparing sprayed and casted electrodes; in both cases, the values for the specific capacitance stayed within a range of just ±5%, illustrating the high reproducibility of the method.

Comparing only the two most promising binders, namely PVP and PTFE in PC and ACN, the rate handling shows a slightly better relative power performance for AC–PVP (capacitance −19% at 10 A g^{-1} compared to −21% for AC–PFTE; see Fig. 7C). The interesting aspect is that the rate handling is comparable to PTFE although the electrode density is much lower and the electrical film resistance is actually higher (AC–PTFE: 0.611 ± 0.02 g cm^{-3}, AC–PVDF: 0.458 ± 0.03 g cm^{-3}, AC–PVP: 0.473 ± 0.01 g cm^{-3}). This behavior is probably related to the optimized electrode/current collector interface as a result of the casting process compared to rolling.

Floating is a reliable method to address the electrochemical stability near the stability window (Fig. 7D). When we first compare the performance of AC–PTFE (which is known for its very high stability; Ref. [43]) and AC–PVP, we see that after 60 h at 2.7 V the capacitance has more severely dropped for PVP-based electrodes using PVP in ACN (−33%) rather than PC (−12%). The AC–PTFE electrode, however, has maintained a high performance at a level of 95% of the initial cell capacitance. Yet, slightly decreasing the maximum operation voltage from 2.7 V to 2.5 V (i.e., mitigating the issues caused by approaching the electrochemical stability window limit) significantly improves the performance stability and a capacitance loss of only 7% is encountered for AC–PVP in ACN (Fig. 7D). This shows the importance of adjusting the maximum cell voltage or, as an advanced tool to mitigate stability limitations, to adjust the mass of both electrodes so that the operational voltage can be maximized [1,44]. We note that decreasing the cell voltage from 2.7 V to 2.5 V in ACN (i.e., −7%) somewhat decreases the energy density from 23.8 Wh kg^{-1} to 20.4 Wh kg^{-1} (i.e., −14%). Qualitatively, the same trends are observed when the performance stability is evaluated by galvanostatic charge and discharge cycling at 3 A g^{-1} (Fig. 7E). While the capacitance decrease after 10.000 cycles is largest for AC–PVP using ACN and a maximum cell voltage of 2.7 V, this decrease (−19%) is less pronounced compared to voltage floating at 2.7 V for 50 h (−29%). This illustrates the less strenuous testing conditions during galvanostatic cycling compared to voltage floating and the enhanced electrochemical degradation in the latter case. Also, it is important to note that the performance decrease for systems with a high electrochemical stability (i.e., AC–PVP in PC at 2.7 V, AC–PVP in ACN at 2.5 V, and AC–PTFE in either ACN or PC at 2.7 V) showed after 50 h of voltage holding a much lower decrease in capacitance (<10%) compared to galvanostatic cycling over 10.000 cycles (12–16%). The cycling stability of AC–PVP at 2.7 V is highly comparable to the PVDF based system, indicating that our much easier fabrication process leads to comparable stability values.

The optimum operational voltage was further investigated using a three electrode cell with AC as the reference electrode and an oversized AC counter electrode (Fig. 8). From successively increasing the electrode potential (versus carbon), following the procedure outlined in Refs. [34,45], it is possible to derive the so-called *S*-value defined as:

$$S_+ = \frac{Q_+}{Q_-} - 1 \text{ and } S_- = \frac{Q_-}{Q_+} - 1$$

with *Q* as the charge and the signs identifying positive or negative polarization; [45] *Q*, in these cases, was calculated from sweeping to various positive and negative electrode potentials in 100 mV increments. In ACN and PC a value very close to −2.4 V versus carbon was identified in both cases for $S = 0.1$ which is a the cut-off criterion for the electrochemical window according to Xu et al. [45]. For positive polarizations, however, we see that the cut-off is reached much earlier for ACN (+1.3 V versus carbon), while PC reaches this threshold at higher voltages (1.5 V versus carbon). These determined values would correspond to a possible cell voltage of above 3.5 V, which according to Fig 7D is definitely not the stability limit of the system. The change in slope in the *S*-value vs. vertex voltage plot in positive direction can be clearly seen at a potential of about 0.75 V vs. carbon, whereas in negative direction, ACN and PC electrolytes behave differently. While PC shows a horizontal line nearly down to a potential of −1.75 V vs. carbon, a constant slope starts for ACN below a voltage of −0.75 V vs. carbon, with a strong increase below −1.75 V vs. carbon. The voltage holding experiments in ACN based electrolytes to 2.5 V cell voltage indicate that the system is stable in this voltage range. Since the voltage window is strongly asymmetric, an adaption of the masses of the positive and negative electrodes might help to further increase the stability. Yet, a stable performance at 2.5 V, as shown by floating, can be reached for AC–PVP in ACN even in symmetric arrangement. The charge/discharge measurements, however, indicate that the degradation mechanism is prone to cycling, meaning that also in PC a slightly lower cell voltage or an adjustment of the electrode masses should be taken into account.

4. Conclusions

In our study, we have shown that PVP can be used as a binder for EDLC electrodes operating in propylene carbonate based electrolyte. Mechanical stability and film integrity increased with increasing molecular mass of PVP; however, considering its electrical isolative behavior and added dead mass, a compromise in PVP content was found to be 3.5 mass%. This amount of PVP (using $M_w = 1.300.000$ g mol^{-1}) showed a negligible impact on total pore volume, average pore size, and resulting specific surface area while enabling drain casting and spray coating directly onto aluminum current collectors.

Vibrational spectroscopy showed readily occurring chemical reactions at room temperature in ACN stemming from traces of residual water. Yet, for PC and ACN, no intrinsic chemical reactions with PVP itself are detected. These findings are in agreement with the electrochemical performance, where AC–PVP electrodes perform comparably well as AC–PVDF (10 mass% binder) or AC–PTFE (5 mass% binder) electrodes under floating to ascertain the electrochemical stability (i.e., stress testing). In case of ACN,

very high performance stability can be observed after extended floating when the maximum cell voltage is decreased from 2.7 V to 2.5 V in agreement with the calculated S-values from sweeping the vertex potentials. Thus, PVP presents itself as a highly suitable binder material for ACN and PC with further room of improvement in future studies dedicated to mass balancing and optimization of cell voltages.

With the higher specific capacitance compared to AC–PVDF and energy ratings only slightly less than AC–PTFE, AC–PVP enables a much more facile production: in contrast to PTFE, the films can be casted or sprayed directly on a current collector and in contrast to PVDF, ethanol can be used instead of toxic NMP as the solvent for slurry preparation. Thus, a fluorine-free binder material, namely PVP, has been shown to be as versatile in casting/spraying as PVDF and such film coating processes can, in addition, be based on a much "greener" synthesis approach.

Acknowledgments

The INM is part of the Leibniz Research Alliance Energy Transition (LVE). We acknowledge funding from the German Federal Ministry for Research and Education (BMBF) in support of the nanoEES^{3D} project (award number 03EK3013) as part of the strategic funding initiative energy storage framework and thank Prof. E. Arzt (INM) for his continuing support. The authors thank K.-P. Schmitt for his support with micro scratch measurements and M. Zeiger for carrying out Raman spectroscopy (both at the INM).

References

[1] F. Beguin, V. Presser, A. Balducci, E. Frackowiak, Adv. Mater. 26 (2014) 2219–2251.
[2] Z. Yang, J. Zhang, M.C.W. Kintner-Meyer, X. Lu, D. Choi, J.P. Lemmon, J. Liu, Chem. Rev. 111 (2011) 3577–3613.
[3] J.R. Miller, Science 335 (2012) 1312–1313.
[4] M. Inagaki, H. Konno, O. Tanaike, J. Power Sources 195 (2010) 7880–7903.
[5] D.B. Robinson, J. Power Sources 195 (2010) 3748–3756.
[6] A. Burke, J. Power Sources 91 (2000) 37–50.
[7] P. Simon, Y. Gogotsi, Nat. Mater. 7 (2008) 845–854.
[8] B. Scrosati, J. Garche, J. Power Sources 195 (2010) 2419–2430.
[9] F. Beguin, E. Frackowiak, Supercapacitors, Wiley, Weinheim, 2013.
[10] Y. Zhai, Y. Dou, D. Zhao, P.F. Fulvio, R.T. Mayes, S. Dai, Adv. Mater. 23 (2011) 4828–4850.
[11] B. Fang, L. Binder, J. Phys. Chem. B 110 (2006) 7877–7882.
[12] R. Kötz, P.W. Ruch, D. Cericola, J. Power Sources 195 (2010) 923–928.
[13] R. López-Chavéz, A.K. Cuentas-Gallegos, J. New. Mater. Electrochem. Syst. 16 (2013) 197–202.
[14] B. Dyatkin, V. Presser, M. Heon, M. Lukatskaya, M. Beidaghi, Y. Gogotsi, Chemsuschem 6 (2013) 2269–2280.
[15] M. Reisch, Chem. Eng. News Archive 86 (2008) 32.
[16] V. Ruiz, C. Blanco, M. Granda, R. Menéndez, R. Santamaría, J. Appl. Electrochem. 37 (2007) 717–721.
[17] A. Garcia-Gomez, P. Miles, T.A. Centeno, J.M. Rojo, Electrochem. Solid-State Lett. 13 (2010) A112–A114.
[18] J. Chmiola, C. Largeot, P.L. Taberna, P. Simon, Y. Gogotsi, Science 328 (2010) 480–483.
[19] V. Presser, L. Zhang, J.J. Niu, J. McDonough, C. Perez, H. Fong, Y. Gogotsi, Adv. Energy Mater. 1 (2011) 423–430.
[20] S. Dhara, P. Bhargava, J. Am. Ceram. Soc. 84 (2001) 3048–3050.
[21] A. Yoshida, K. Imoto, Electric Double Layer Capacitor and Method for Producing the Same, 5,150,283, U.S.P. Office, 1991.
[22] S. Barusseau, F. Martin, B. Simon, Liant pour électrode de système électrochimique à électrolyte non aqueux, Binder for Electrode of an Electrochemical System Employing a Non-aqueous Electrolyte, EP 0 907 214 B1, E.P. Office, 1998.
[23] C. Portet, P.L. Taberna, P. Simon, C. Laberty-Robert, Electrochim. Acta 49 (2004) 905–912.
[24] N. Böckenfeld, S.S. Jeong, M. Winter, S. Passerini, A. Balducci, J. Power Sources 221 (2013) 14–20.
[25] L. Vaisman, H.D. Wagner, G. Marom, Adv. Colloid Interface Sci. 128–130 (2006) 37–46.
[26] Y.L. Hsin, K.C. Hwang, C.-T. Yeh, J. Am. Chem. Soc. 129 (2007) 9999–10010.
[27] A.V. Neimark, Y. Lin, P.I. Ravikovitch, M. Thommes, Carbon 47 (2009) 1617–1628.
[28] S. Brunauer, P.H. Emmett, E. Teller, J. Am. Chem. Soc. 60 (1938) 309–319.
[29] Bestimmung der spezifischen Oberfläche von Festkörpern mittels Gasadsorption – BET-Verfahren (ISO 9277:2010), 2014.
[30] BSI British Standards, Determination of the Specific Surface Area of Solids by Gas Adsorption – BET Method, ISO/DIS 9277, ISO/DIS 9277, 2008.
[31] D. Weingarth, A. Foelske-Schmitz, A. Wokaun, R. Kötz, Electrochem. Commun. 18 (2012) 116–118.
[32] D. Weingarth, A. Foelske-Schmitz, R. Kötz, J. Power Sources 225 (2013) 84–88.
[33] M.D. Stoller, R.S. Ruoff, Energy Environ. Sci. 3 (2010) 1294–1301.
[34] D. Weingarth, H. Noh, A. Foelske-Schmitz, A. Wokaun, R. Kötz, Electrochim. Acta 103 (2013) 119–124.
[35] P.W. Ruch, D. Cericola, M. Hahn, R. Kötz, A. Wokaun, J. Electroanal. Chem. 636 (2009) 128–131.
[36] P. Lespade, R. Al-Jishi, M.S. Dresselhaus, Carbon 20 (1982) 427–431.
[37] M.A. Pimenta, G. Dresselhaus, M.S. Dresselhaus, L.G. Cancado, A. Jorioa, R. Saitoe, Phys. Chem. Chem. Phys. 9 (2007) 1276–1291.
[38] M. Hayama, K.-I. Yamamoto, F. Kohori, T. Uesaka, Y. Ueno, H. Sugaya, I. Itagaki, K. Sakai, Biomaterials 25 (2004) 1019–1028.
[39] K.S.W. Sing, D.H. Everett, R.A.V. Haul, L. Moscou, R.A. Pierotti, J. Rouquerol, T. Siemieniewska, Pure Appl. Chem. 57 (1985) 603–619.
[40] J. Rouquerol, D. Avnir, C.W. Fairbridge, D.H. Everett, J.M. Haynes, N. Pernicone, J.D.F. Ramsay, K.S.W. Sing, K.K. Unger, Pure Appl. Chem. 66 (1994) 1739–1758.
[41] L.S. Taylor, F.W. Langkilde, G. Zografi, J. Pharm. Sci. 90 (2001) 888–901.
[42] P. Kurzweil, M. Chwistek, J. Power Sources 176 (2008) 555–567.
[43] P.W. Ruch, D. Cericola, A. Foelske, R. Kötz, A. Wokaun, Electrochim. Acta 55 (2010) 2352–2357.
[44] A. Brandt, P. Isken, A. Lex-Balducci, A. Balducci, J. Power Sources 204 (2012) 213–219.
[45] K. Xu, S.P. Ding, T.R. Jow, J. Electrochem. Soc. 146 (1999) 4172–4178.
[46] G. Socrates, Infrared and Raman Characteristic Group Frequencies: Tables and Charts, third ed., John Wiley & Sons. Ltd., Chichester, 2004.
[47] J.E. Schaff, J.T. Roberts, Langmuir 15 (1999) 7232–7237.